

Automation of Data Acquisition in Transient Photoconductive Decay Experiments

Abstract: The application of a time-shared IBM 1800 Data Acquisition and Control Computer to data acquisition and reduction in transient photoconductive decay experiments is described. These experiments present an interesting problem in laboratory automation, since they involve high data rates (data periods frequently on the submillisecond scale), a free-running independent variable (time), and a mode of operation in which it is possible to amass large quantities of data in a relatively short time. Techniques are described wherein these transient data are collected in real time while the computer simultaneously monitors many timer-based, slower-scanning experiments. The computer is shown to facilitate a variety of otherwise formidable data manipulation and analysis tasks. In addition to improving the quality of the data obtained, automation of these measurements provides data analysis and display of physical results within minutes after each data logging run, permitting the experimenter to interact closely with the data in a fashion not possible under manual operation.

Introduction

Phototransport phenomena are now widely studied in solid state physics, both as a tool for the investigation of the intrinsic and extrinsic internal electronic processes in semiconductors and insulators, and for the application in a variety of devices, e.g., radiation detectors, television imaging devices, and electrostatic copiers. Since phototransport involves a combination of two more basic processes, optical excitation and electrical transport, experiments in this field involve a relatively large number of variables or parameters. For example, one may vary the intensity or photon energy of the exciting illumination, the magnitude or sign of the applied potentials, and the temperature. In addition, experiments may be performed with electrical or optical stimuli of a dc, ac, or fast pulse nature. In this kind of experimental situation large quantities of data may be amassed and prodigious amounts of arithmetic manipulation required before all of the physical information can be extracted from a given set of measurements.

This paper describes the automation of the data collection in a particular photoconductivity study in the IBM San Jose Research Laboratory and, to our knowledge, reports the first application of laboratory automation to the study of phototransport phenomena. The experimental apparatus is briefly described and the rationale for automating it is discussed. The automated system is then described, including several examples of the degree to which on-line data handling capability has

been developed. Finally, some remarks are made concerning natural extensions of the present system.

Many instances may be cited of laboratory automation applications involving data rates as high as those used in the present work. Often in such cases an on-line computer is totally dedicated to the experiment[1,2] and/or use is made of special high-speed analog-to-digital converters, multichannel analyzers, and buffer storage[1-3]. The present application is an example of the use of a medium-sized, time-shared computer to simultaneously monitor slow-scanning and high-data-rate experiments without the need for specialized interface hardware. Okaya[4] has reported the monitoring of high-data-rate flash photolysis experiments and a variety of slow-scanning chemistry experiments with a single process-control computer. The system used in that work is interrupt driven, with the computer acting as a slave to each on-line experiment. Hence, the problems encountered are very different from those of the present application, wherein the slow-scanning monitor is timer based and both the fast experiment and many of the concurrent slow experiments may be time dependent. A fuller discussion of these matters is given in Ref. 5.

Experimental configuration

The photoconductive measurements involved in this work form one part of a larger effort in our laboratory to characterize and understand the photoelectronic behav-

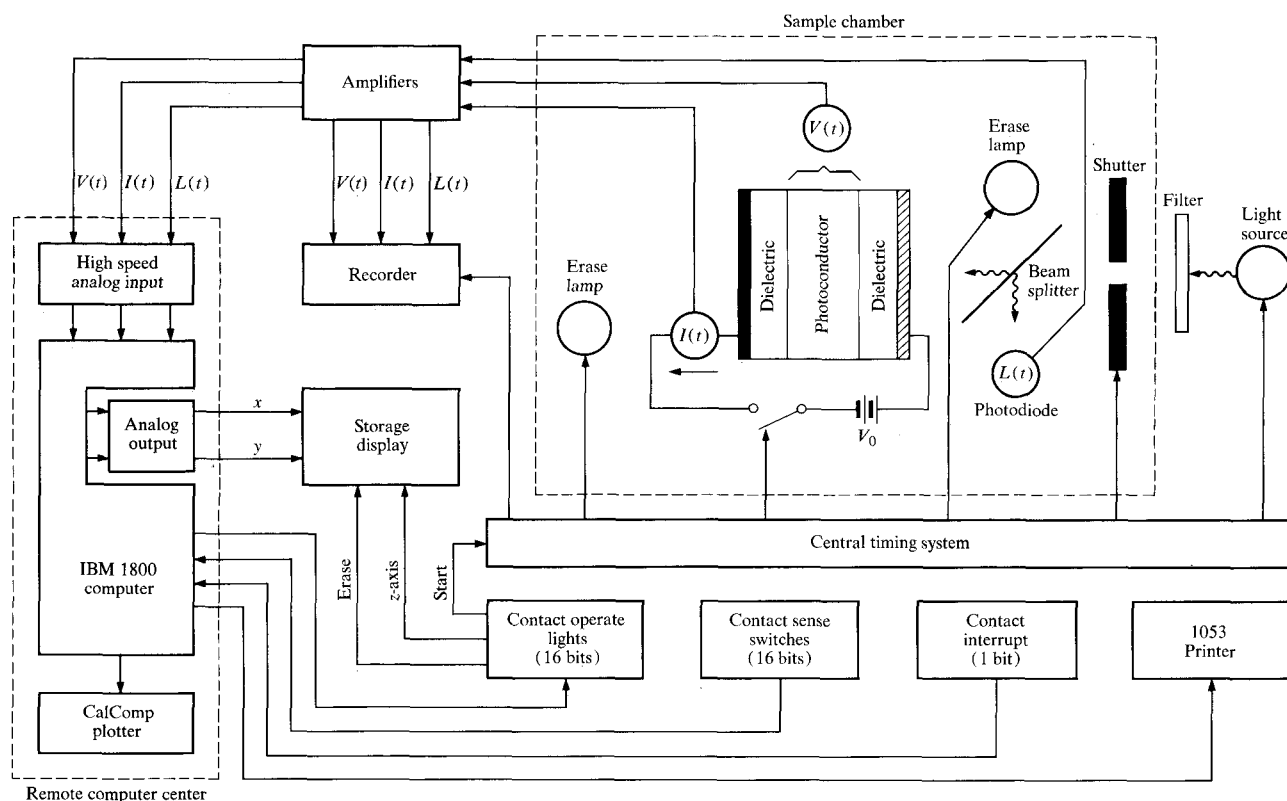


Figure 1 Block diagram of the hardware configuration for the automated transient photoconductivity experiments.

ior of new and interesting materials. The photoconductor sample itself is sandwiched together with one or two layers of dielectric between metallic contacts, as shown in Fig. 1. At least one of the contacts is made semitransparent to permit irradiation. This sandwich configuration, in which electronic transport takes place parallel to the direction of incoming radiation, is of interest for a number of reasons. For basic scientific studies a geometry similar to this, but usually with vanishingly thin dielectrics or none at all, is used to measure carrier drift mobilities[6]. Recent work has made possible the interpretation of such measurements for configurations with thicker dielectrics[7,8] and has provided new means for obtaining information about carrier lifetimes and trapping times from the measurements[9]. From an applications point of view, the thick dielectric sample configuration of Fig. 1 allows one to study the behavior of the photoconductor under device-like situations in which the voltage across the sample is a decaying function of time. Such would be the case in imaging or electrophotographic applications. Furthermore, the presence of the dielectric layers enables one to investigate in a controlled manner the effects of various metallic contacts on the photoconductor properties.

Shown in Fig. 1 are the key features of the instrumentation used in these measurements. The heart of the

apparatus is the central timing system, which consists of eight identical hardware timers with selectable on-times from 0.001 to 255 sec. The sequencing of the eight timers is totally flexible. These timers are used to control the other apparatus illustrated in Fig. 1, i.e., to open a 135-mm Graflex, 1000 shutter, trigger the flash lamp, activate the tungsten-halogen "erase" lamps (250 W), drive the recorder chart, turn on the field, etc. In a typical experimental sequence, an initial nulling procedure is followed by application of a potential V_0 across the entire sandwich in the dark. The potential at first divides between the photoconductor and the dielectric(s). Because of the finite dark conductivity of the photoconductor, a current $I(t)$ flows in the external circuit and $V(t)$, that portion of V_0 which appears across the photoconductor, diminishes with time. The sample is subsequently illuminated with either flash or step-function light passed through an optical system consisting of two lenses and an Optics Technology narrow-band interference filter. The light generates carriers in the photoconductor and an increased contribution to $I(t)$ is observed. Correspondingly, the decay of $V(t)$ occurs more rapidly in the presence of illumination. The data to be recorded during this process consist of the external current $I(t)$, the voltage $V(t)$ across the photoconductor, and the illumination $L(t)$, all as functions of time, the independent variable. Since electrode contact

is not made to both surfaces of the photoconductor, $V(t)$ is measured by incorporating the sample sandwich into a capacitive bridge and using a preamplifier with high input impedance in the measurement arm of the bridge. The "erase" lamps shown on either side of the sample provide intense white light and produce a null condition in this bridge circuit. The illumination signal is recorded using the current through an RCA Model 926 photodiode which monitors the light reflected from a beam-splitter. Calibration of the photodiode is done with an Eppley thermopile. The $L(t)$ data are recorded as the instantaneous incident photon flux density in the case of step-function illumination and as the integrated incident-photon flux density in the case of flash illumination. The $V(t)$, $I(t)$ and $L(t)$ signals are fed through amplifiers before recording. The chart recorder, using multiple optical galvanometric pens, records all three signals and simultaneously records accurate time bars onto its chart paper, with an ultimate resolution of about 1 msec.

With the apparatus depicted in Fig. 1 it is possible to run many experiments within a short period of time. A typical run of the type described takes at most a few seconds, and the setup time for a subsequent run is rarely longer than several minutes. It is therefore possible to vary some parameter (e.g., the wavelength of the irradiation) and in one or two hours collect a large set of unreduced data. The complete manual analysis of such data could require several days of tedious manipulation (e.g., to calculate and plot the field dependence of the carrier photoinjection efficiency at each wavelength) before all the final physical results were displayed, whereas the automated data analysis can be performed quasi-interactively. It is primarily for this reason that the benefits of computerized data handling seemed most attractive in the present application. In the following section we discuss in detail the several limitations imposed by operating experiments of this type in a manual mode. As will be seen, many subsidiary benefits accrue once the initial stages of the automated system have become operational.

Limitations before automation

Manual operation of the transient photoconductivity experiments described in the previous section imposes two major types of limitation on the amount of data that can be collected and the degree to which the data can be analyzed. First there is a limitation associated strictly with the quality of the recorded data. The response time requirements of the recording system exclude the use of conventional potentiometric x - y recorders. Recorders that use optical writing on photosensitive chart paper provide improved response time but at a sacrifice in record quality. The records are of limited resolution in the dependent variables because of small chart width and are

of relatively short useful lifetime because of degradation of the image in light. Furthermore, time resolution better than the 1 msec limitation of the optical galvanometer would be desirable. These factors can be overcome with installation of more sophisticated recording hardware but only at significant expense.

The second and by far more severe limitation met under manual operation is the inordinate amount of time that must be spent on data reduction, as already pointed out. Such operation effectively precludes any interactive form of experimentation wherein one chooses interesting phenomena to study in detail in subsequent runs based on an analysis of the preceding run. After data reduction is completed manually, even simple modifications or extensions of the analysis (e.g., a change in graph scaling) require a fair amount of additional labor. For more complicated extensions of the analysis (e.g., matching of the experimental results to theoretical predictions) one may have to resort to the tedious manual conversion of the data to digital form for use in computation.

It will be seen that the automation of this experiment alleviates to a great extent the problems cited here. It is worth noting that the discussion in the preceding paragraph is of a quite general nature, and that these sorts of problems arise in any experimental situation where the time required to accumulate data is small compared to the time required to subsequently process the data. It is fair to say that a large number of physics experiments fall into this category.

Automated transient photoconductivity measurements

Once the decision to automate an experiment is made, the aspects of the apparatus to be automated must be determined. In the present case, since sophisticated control hardware existed in the laboratory in the form of the central timing system, it was judged unnecessary to use the computer to control the actual sequencing of the experimental procedure. The automation package described here therefore consists primarily of a collection of programs and a hardware interface designed to acquire the $V(t)$, $I(t)$ and $L(t)$ data and to perform data reduction, analysis and display functions. Since the transient photoconductivity experiments may involve numerous permutations of the parameters under study, it becomes difficult to plan the programming to cover all data handling situations that may arise. The approach chosen here is to make the data acquisition phase of the experiment as general as possible, and to handle specific data analysis problems with individually specialized task programs. The working details of this approach will be clear from the discussion that follows.

The programs described were developed and have been used on an IBM 1800 with an operating system

designed within the IBM-supplied Time Shared Executive (TSX) package [10]. The reader is referred to Ref. 10 for a thorough description of the system hardware and software configuration. Some familiarity with 1800-TSX terminology is assumed in the discussion that follows. A second version of our programs has recently been implemented to run under the Multiprogramming Executive (MPX) package which is the current operating system on our computer. The 1800 in our laboratory is presently servicing 15 experiments. Most of these are of a generalized spectroscopic nature and use the 1800 in a time-sharing mode. Since the data rates in these spectroscopic experiments are anywhere from 125 to 80,000 times slower than the fastest data rates used in the automated transient photoconductivity studies, some new problems had to be solved and a method of interleaving the high- and low-data-rate experiments had to be developed. Stated briefly, the operational scheme adopted was that a high-data-rate experiment could mask the slower experiments and in effect see a dedicated 1800, but only for a period such that none of the time-sharing experiments would lose more than four data points. In practice on our system the masking time allowed for high-data-rate experiments falls in the range between 2 and 15 sec. A more detailed discussion of the problems of interleaving fast and slow experiments on a timer-based laboratory automation monitor system is given by Grant[5].

The operation of our automated transient photoconductivity experiments divides naturally into three phases: a run initialization phase, a data acquisition phase, and a data reduction and analysis phase, as depicted in Fig. 2. Run initialization consists of communicating to the computer a set of parameters containing information necessary for the data logging and subsequent analysis. Then, once the data are collected, any of several data handling tasks may be placed in the TSX queue and then executed. These may perform the functions of validity-checking the run parameters and the data, reducing the data, and providing results on a storage display, paper plotter, or character printer. After viewing the results of these data handling operations, the experimenter in his laboratory can selectively alter certain features of the computations and rerun the tasks, thereby achieving a degree of quick-response, interactive manipulation of the data. The various phases of the automated photoconductivity work shown in Fig. 2 are discussed more fully in the following sections.

• *Laboratory-computer interface*

The simple interface hardware constructed for laboratory-computer communication consists of a set of linear amplifier circuits for conditioning the analog input/output signals and a collection of toggle switches and lamps to handle digital input/output. The analog input

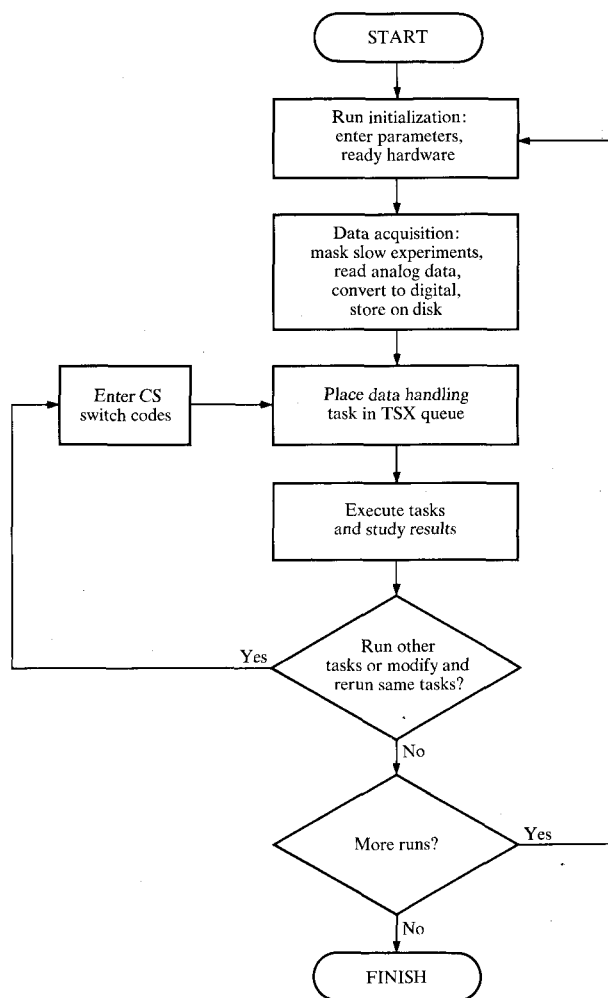


Figure 2 Flowchart illustrating typical mode of operation of the automated experiments.

signals are brought to the 1800 differentially over shielded twisted pair cable and fed through unity-gain differential amplifiers to the high-level solid state multiplexer and analog-to-digital converter (ADC). The analog output signals are handled similarly, with unity-gain differential amplifiers coupling them to the *x* and *y* inputs of a Tektronix 611 storage display. In addition, moderate quantities of printed output are obtained in the laboratory on an IBM 1053 printer. Digital input consists of a set of 16 switches connected to a contact sense (CS) group of the 1800. These switches are used to communicate command codes to the computer or to enter parameter values. Digital output is indicated by a set of 16 lamps driven by a contact operate (CO) group and is used to display signals from the computer to indicate that a parameter has been read, a given task completed, or other key information. Certain individual bits of this digital output group are used to control the ERASE, Z-

Table 1 Parameters used in the automated photoconductivity experiments.

Hexadecimal number	Parameter function	Type ^a
0001	Data-handling task selection	M
0002	Total scan time (to nearest 0.01 sec)	C
0003	Number of data points	C
0004	Delay period (to nearest 0.01 sec)	C
0005	Sample area	M
0006	Sample thickness	M
0007	Date	B
0008	Data set number	B
0009	Balance capacitance	M
000A	First applied voltage	M
000B	Second applied voltage	M
000C	Run number	B
000D	Wavelength or dark-run flag	M
000E	Current scale factor	M
000F	Irradiation scale factor	M
0010	Voltage scale factor	M
0011	Printer designation	M
0012	Computation and printing control	M
0013	Smoothing and plotting control	M
0014	Plotting control	M

^aB = bookkeeping, C = run control and M = data manipulation parameter. Parameters 0001, 0012, 0013 and 0014 have the special feature that they may be altered at will at any time after data acquisition and thereby can be used to interact with the data-handling task programs.

AXIS and VIEW modes of the storage display and to trigger the central timing system when the computer is ready to initiate data acquisition. At all times the computer's "attention" is gained by calling into core an interrupt coreload associated with an 1800 contact interrupt (CI) level that is wired to the laboratory. This coreload (named GONET) first reads the 16 CS switches and then takes action depending on the switch code read. The CS and CI switches and the CO lights are shown schematically in Fig. 1 as part of the hardware configuration in the laboratory. The digital portion of the hardware interface unit is quite similar to the interface unit depicted in Fig. 5 of Ref. 11.

• Run parameter entry

The parameters used in the run initialization phase of the photoconductivity experiments are listed in Table 1. Twenty parameters are shown and their hexadecimal identification numbers indicated. The list can be categorically divided into three types of parameters: bookkeeping, run control, and data manipulation, as shown in the table. Bookkeeping parameters serve to uniquely identify a particular run, an important function when large quantities of data are collected. Run control parameters define the data logging rate of the run and provide for the synchronization of the data acquisition with the appropriate hardware processes (controlled by the central timing system) in the laboratory. Data manipulation pa-

rameters specify information needed for data reduction, analysis and display. Although the parameter list in Table 1 may seem long, one must realize that, for a typical data set, most parameters remain fixed while only one or two are altered from run to run, e.g., run number and wavelength. Furthermore, parameter entry has been greatly facilitated by making provision for binary coded decimal entries and for editing one or a few parameters without altering the others in the list.

• Data acquisition

Once the run initialization is complete, a special signal is entered into the CS switches and the interrupt coreload GONET is summoned to perform the data acquisition function. It is here that one encounters some of the more novel aspects of our particular automation application, and these are noted below. The following discussion refers to the highly schematic flow-chart of GONET shown in Fig. 3.

Upon entry, GONET first reads the 16 CS switches and then, depending on the switch code read, branches to perform data collection or any of several utility functions. If the signal to begin data acquisition has been entered, much programmed activity occurs before the data scan actually begins (see Fig. 3). Since several other experiments may be simultaneously active on the 1800, with individual data rates up to 20 points/sec, this pre-scan activity must include testing of the requested total scan time (as given in parameter 2) to ensure that no concurrent experiment would lose more than four data points. If all tested parameters are within appropriate limits, one bit of the CO group is used to initiate the hardware timer sequence in the laboratory. This single action represents the only degree of control exercised by the 1800 during the entire data collection phase of our experiment. Once the timing system has been triggered, the requested delay period (if any) before data collection begins is counted down in an assembler subroutine STALL. This subroutine also determines whether the actual real-time delay period does not exceed the requested delay time by more than a specified limit (typically 50 msec). Such checking is necessary in the event that some occurrence (e.g., the emptying to disk of a core buffer used by a background time-sharing experiment) detains the delay countdown just before its completion. In practice it appears that this situation has never been encountered on our system. Finally, on exiting from STALL, the validity-check on the requested masking time is repeated to ensure that no experiments that would suffer a loss of more than four data points have been initiated during the delay. Again, this validity-check on masking rarely, if ever, indicates, failure.

At this stage GONET calls for SLURP, an assembler language subroutine used to mask all the 1800 interrupt

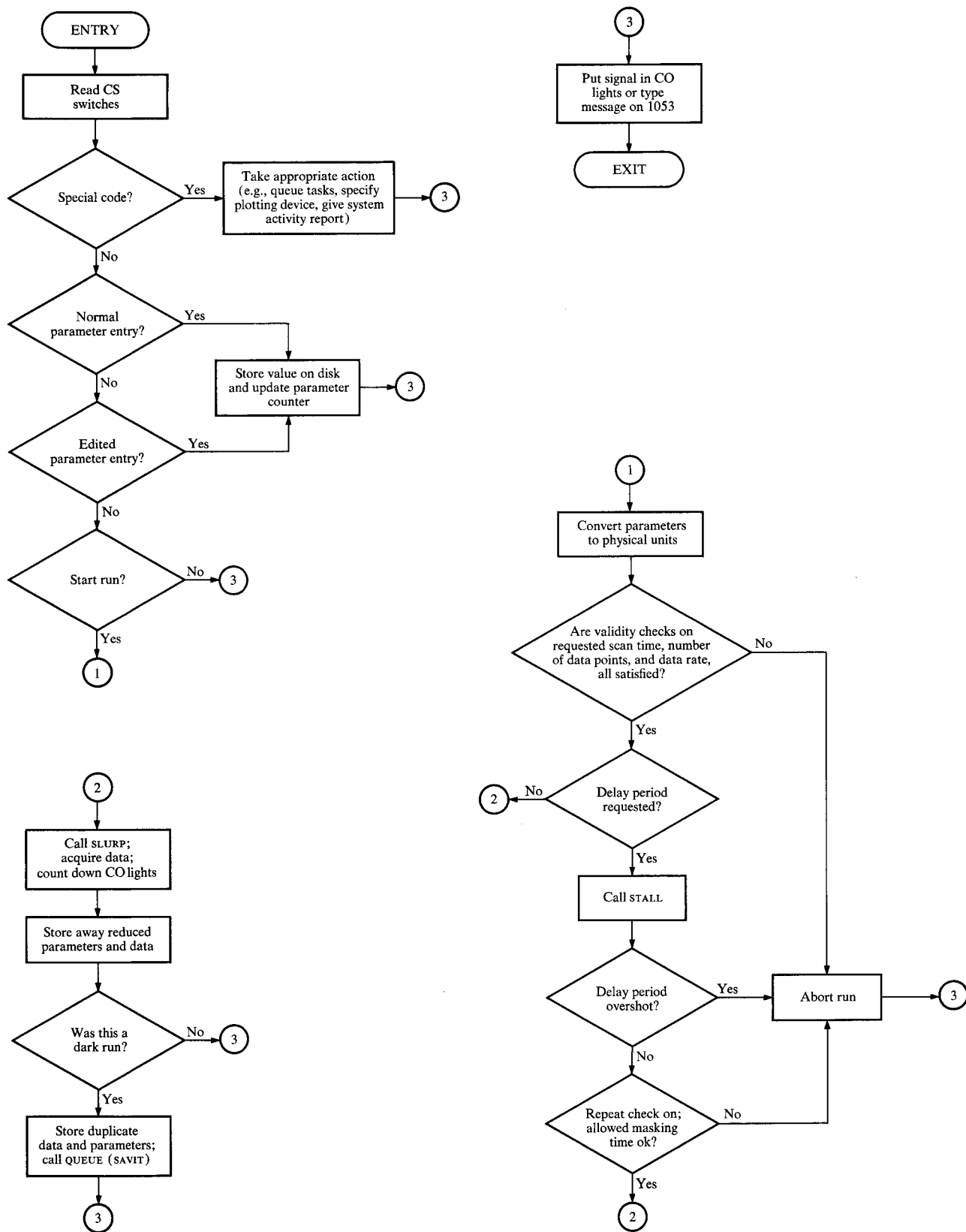


Figure 3 Schematic flowchart of the interrupt coreload GONET used to read the run parameters, to acquire and store data, and for several utility functions.

Table 2 Summary of data handling tasks used in the automated photoconductivity experiments.

Task	Function	Principle output
1	Display parameters in physical units	IBM 1053 printer
2	Scale and display raw data	Storage display CalComp plotter
3	Reduce data and display physical results when using step-function illumination	Storage display CalComp plotter 1053 printer
4	Validity-check $I(t)$ vs $V(t)$	Storage display CalComp plotter
5	Reduce data and display physical results when using pulse illumination	1053 printer

levels and to read the data at a fixed rate, as computed from parameters 2 and 3. The analog input multiplexer is capable of sampling rates up to 24 kHz, and the conversion rate of the analog-to-digital converter (ADC) using 14-bit resolution is about 23 kHz. Because of settling time the maximum system conversion rate is somewhat slower. The $V(t)$, $I(t)$ and $L(t)$ signals are read under program control from three sequential analog input addresses, and the timing of each set of three READ operations is achieved using one of the 1800 hardware timers with a time base of 125 μ sec. A fixed data-acquisition rate without interruption is assured because of the masking of all interrupts. The ultimate limitation in our data transfer rate is imposed by a combination of the hardware specifications mentioned above and the programming overhead in SLURP. The shortest data period attainable in the present work corresponds to three counts of the hardware timer, or 375 μ sec. This represents an over-all data transfer rate (i.e., for all three dependent variables) of 2.7 kHz, or an individual data rate of 8 kHz. Our system thus allows the collection of 500 sets of data points during a transient photodecay experiment with a scan time as fast as 187 msec or as slow as 15 sec. All this occurs while the computer suspends many slower-scanning experiments, with essentially no deleterious effects on those scans.

Upon the exit from SLURP, the parameter list (in physical units) is stored on disk for use in data handling routines. Then the $V(t)$, $I(t)$ and $L(t)$ arrays present in core are written onto disk for later access. This is done using the integer format in which the raw data is obtained from the ADC. In order to economize on disk space requirements and to minimize the execution time of the interrupt coreload GONET, no conversion to floating point or

physical scaling is done at this time. If parameter D has indicated the current data to be for a "dark run," a duplicate set of parameters and $V(t)$ and $I(t)$ integers are stored in a second file on disk for use in conjunction with subsequent "light runs." When a new data set is acquired, both the old parameter and old raw data files are overwritten with new values. This mode of operation is economical of disk space; however, it necessitates completion of all data handling routines before new data are read. A possible departure from this mode of operation is discussed in our remarks on future extensions of the present system.

• Data handling procedures

Once data acquisition and storage are completed, a signal is given in the CO lights to indicate that the data manipulation phase of the experiment may commence. Recall that parameter 1 is reserved for defining data analysis tasks. The operator thus responds by entering in parameter 1 a code indicating the data reduction programs that are to be used. By subsequently entering the appropriate CS switch code and employing the contact interrupt, the selected tasks are placed in the TSX queue and sequentially executed in the specified order (see Fig. 3). The coding allows up to four tasks to be requested in any single entry of parameter 1, and choices for these tasks may be made from among 15 numbered task programs. This procedure provides almost unlimited flexibility for the operator in the queuing of data handling routines.

Presently five such task programs have been written and are described here. The task programs are executed in times ranging from a few seconds up to about 1 min, plus plotting time. All plotting can be directed to either the storage display unit or the paper plotter, depending upon a CS switch code entry. When plots are directed to the storage display, two bits of the CO group are used to control the erase and z-axis turn-on functions. Activation of the z-axis automatically places the display in the view mode immediately before the plot is drawn. The plotting of a single curve (including scale marking and titling) takes about 20 sec on the storage display and roughly 2 min on a CalComp plotter. The complete data handling procedure (involving the execution of several task programs) can be accomplished within 2 to 10 min after a data collection run while the 1800 simultaneously monitors many time-shared experiments. Comparable amounts of manual data manipulation would take on the order of a day to complete, and almost certainly errors would be introduced in the process.

Table 2 summarizes the functions of each of the data-handling task programs. Tasks 1 and 4 serve primarily for validity-checking the acquired data. Task 1 provides laboratory printout of essentially all key parameters

(decoded into physical units) not already displayed in the data collection printout. Task 4 is a utility routine that checks the $V(t)$ and $I(t)$ data for a functional relation between the two, namely that $I(t)$ is equal to the known capacitance of the dielectric layer in the sample sandwich multiplied by the time derivative of $V(t)$. A plot is made of two curves which must be in superposition if the $V(t)$ and $I(t)$ data are physically valid.

Task 2 is predominantly a plotting routine that scales the $V(t)$, $I(t)$ and $L(t)$ data and displays each of these variables as a function of time on either the storage display or the plotter, much in the way these curves appear on the original chart records. Task 2, however, provides the important advantages of labeling and scaling the plots and producing high-resolution, high-quality hard copy not available from the chart. Typically this task is used with the laboratory display unit to examine the data just collected, in order to determine what further data manipulation is advisable.

In Fig. 4 curves plotted by task 2 in a study of a charge transfer, complex organic photoconductor are shown superimposed for a dark run (dashed) and a subsequent light run (solid), as photographed directly from the storage display screen. The curves are, from top to bottom, dark current, light current, light voltage, dark voltage, and instantaneous photon flux density. No labeled axis appears for the flux density curve. Note that the voltage and current traces are negative, with their zeros at the top of the figure. The time scale extends from 0 to 15 sec. At 0.25 sec a voltage $V_0 = -800$ V is applied, and $V(t)$ across the photoconductor jumps from zero to -440 V. This voltage decreases slowly in the dark, with a corresponding monotonic decrease in the dark current from its maximum value of $-0.4 \mu\text{A}$. At 1.27 sec the shutter is opened and beyond this time the dark and light traces diverge. During irradiation, the current increases and $V(t)$ consequently decays at a faster rate. At the end of the run there is a difference of 223 V between the dark and light $V(t)$ curves, and $V(t)$ in the light has decreased to -37 V.

We comment next on task 5 and briefly postpone the discussion of task 3, since that will be done in considerably more detail. The fifth task in Table 2 is a data analysis task specifically oriented to measurements with fast-pulse illumination. In this case the integrated photon flux density is recorded and appears much the same as the instantaneous $L(t)$ function of Fig. 4. The dark and light decay data are analyzed for the degree of voltage decay attributable to the illumination, and this information is used to compute the photoinjection efficiency for the charge carriers under study[9,12].

The third task listed in Table 2 is one that analyzes the data for key physical results and plots reduced results, e.g., the photoconductive quantum efficiency vs

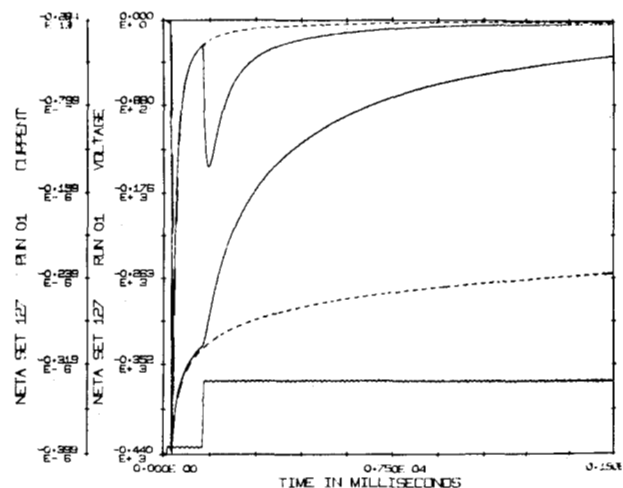


Figure 4 Photograph from storage display screen showing plots of scaled data superimposed from both dark (dashed curves) and light (solid curves) runs. The dashed curves were obtained by modulating the display's z-axis signal with a 15-Hz audio signal. The individual curves are identified in the text.

the electric field strength. This is the most intricate analysis program in the present automation package, since it does much numerical computation and allows for a rather large number of options in its mode of execution.

To demonstrate this point, a simplified flow chart of task 3 is presented in Fig. 5. In practice, task 3 is made up of a smoothing and plotting task coreload chained to a computation task coreload, because the incorporation of all program instructions and subroutines needed for computation, smoothing, and plotting would form a coreload too large for the 16K word variable core size of our 1800. By way of example, assume that the data for the dark and light runs are plotted as shown in Fig. 4. The capability exists to maintain in disk storage a copy of the dark-run data while acquiring subsequent light-run data. Thus two data files exist, one with the light data and one with the dark data, each with its corresponding physical parameter file. Let us further assume that the objective of the analysis is a plot of how the photoconductive quantum efficiency (the number of carriers transported per incident photon) depends on the electric field, with both abscissa and ordinate on logarithmic scales. The steps involved in such a computation are traced in Fig. 5. A more thorough discussion of the details is not within the scope of the present paper. It is worth noting, however, that this calculation of the field-dependent quantum efficiency, including corrections for dark conduction, is a particularly good example of a data analysis computation that can be performed readily with the computer but would be extremely time consuming and likely to be fraught with errors if carried out manually from the chart recorder traces.

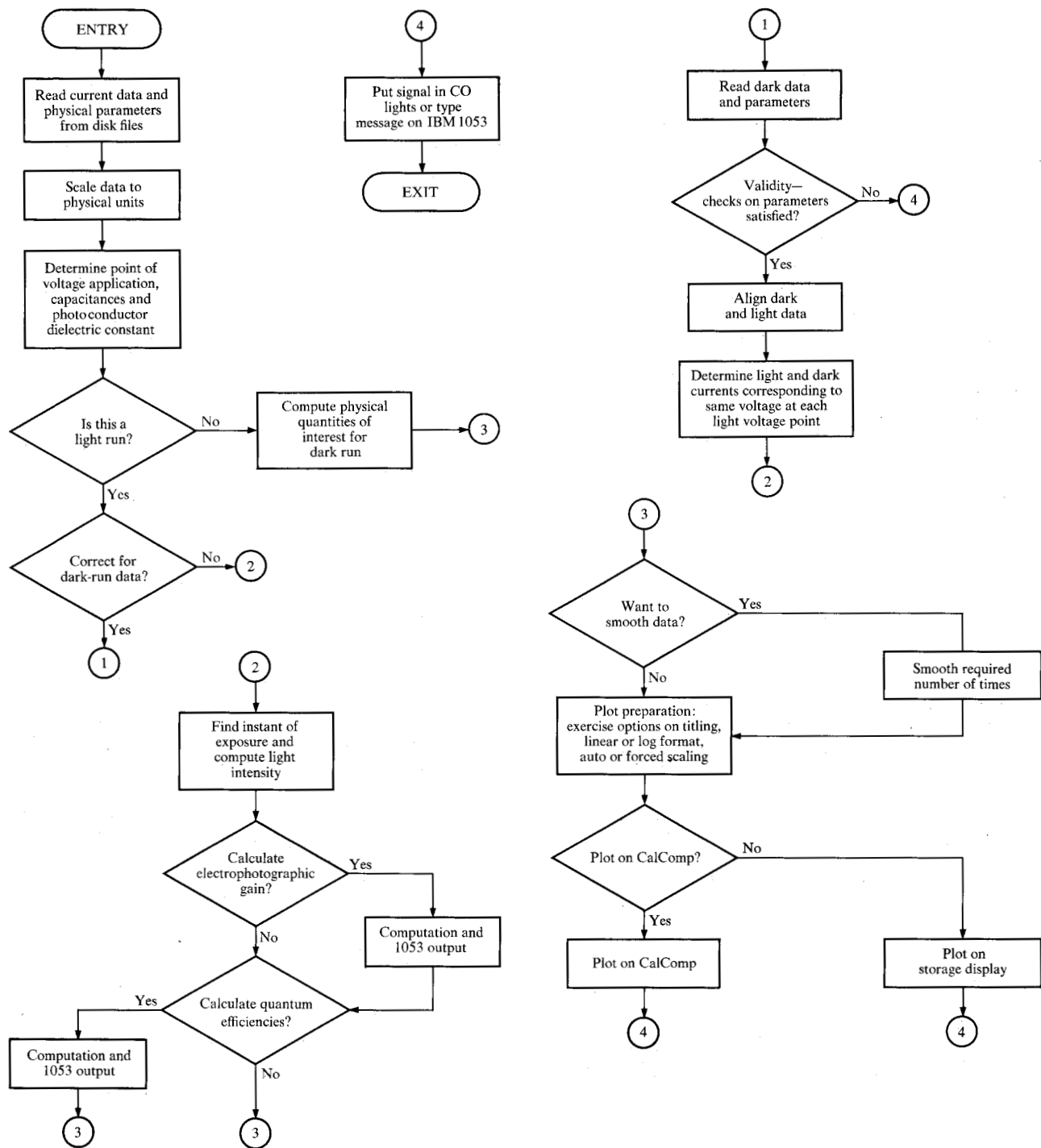


Figure 5 Schematic flowchart of process coreload for data handling task 3.

Beyond the computation of the desired physical quantities, task 3 offers a variety of smoothing and plotting options that are used to display the results most effectively. The exercise of these options is done interactively after data acquisition and storage, so that the experimenter can view reduced results and then alter the

data handling routines to produce reduced results in a more desirable format. The plot-controlling options include a choice of linear or logarithmic scales, of automatic scaling or scaling with externally specified origins and scale factors, and of various titlings for the plot axes, depending on the nature of the data analysis pro-

cedure used. An illustration of a typical plot is shown in Fig. 6, as obtained on the CalComp plotter. The curve of Fig. 6 depicts the quantum efficiency of the photoconductor as a function of the electric field, obtained using the data shown in Fig. 4 and by means of the computation outlined in Fig. 5. It has been shown recently[13] that, under appropriate experimental conditions, such a curve can be interpreted as the photoinjection efficiency of free carriers at the illuminated surface of the photoconductor. This quantity is of considerable physical interest[12]. In Fig. 6 the scales are logarithmic and external scaling has been specified. The ordinate data for the curve were smoothed six times, although an essentially noise-free curve could have been obtained without smoothing in this particular example.

One further point to be made concerns the improvement in actual measurement resolution and signal-to-noise ratio achieved by the automation scheme. The resolution of the $V(t)$, $I(t)$ and $L(t)$ traces on our chart recorder is limited, at best, to one percent of full scale. In fact, since $I(t)$ often varies by several orders of magnitude during a single photodecay, before the automation method was used, it was necessary to use a fast range-switching preamplifier in the current measurement circuit to improve the resolution. This arrangement necessitated the additional labor of catenating $I(t)$ data from several scale ranges during manual data reduction, and often led to systematic errors in the output because of small calibration errors existing on the different ranges. The high resolution of the ADC (in the absence of noise better than 1 part in 10^4 with 14-bit conversion) in our automated operation greatly improves the situation, and the need for range switching no longer exists. Figure 6 shows that the ordinate values derived from the $I(t)$ data vary by nearly two orders of magnitude with very little degradation in signal-to-noise ratio at the weak signal portion of the curve, where $I(t)$ is on the order of 10^{-9} A.

Concluding remarks

We have described the use of an IBM 1800 computer in the automation of transient photoconductivity measurements. The automated experiments are characterized by a wide range of data rates and the method permits the accumulation of large quantities of data in short measurement periods. Furthermore, the data is in a form that requires a great deal of arithmetic manipulation before useful physical results are obtained. This requirement has led to a mode of operation in the automated experiment wherein data is acquired from one experiment while slower experiments which time share the 1800 are masked for a short period. Complete analysis of the acquired data is then performed on-line within a period of minutes. The operational technique allows the experimenter to interact closely with the data and to

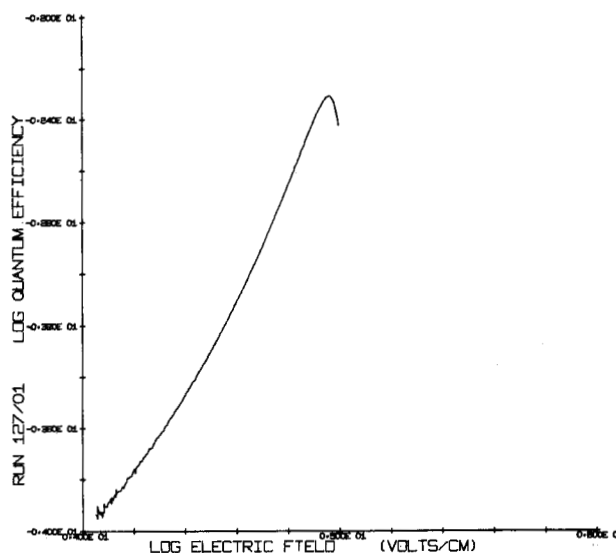


Figure 6 CalComp plotter output on logarithmic scales of the photoconductive quantum efficiency vs the average electric field, as computed from the data in Fig. 4.

make decisions to modify or repeat experiments after viewing reduced physical results, usually in scaled graphical form. Automation has afforded major improvements in the quality and permanence of the hard copy records obtained, plus significant increases in the measurement resolution for both the independent and the three dependent variables. In addition, the detailed analysis of the data (of a degree that would require prohibitive time if done manually) is now done routinely and with a high level of confidence in the results.

There are several ways in which the operation described could be usefully enhanced in the future. Present limitations on disk storage space make it necessary to overwrite the data of each run with the data for the next run and require the kind of complete and immediate on-line analysis described here. In many instances it would be desirable to accumulate data from 10 or 20 runs before carrying out all data handling routines. This could easily be accomplished with adequate storage space for the accumulated data. Concurrently, the capability for storing data from a large number of runs would greatly increase the practicability of transferring the data to a larger computer, either by punch card transcription or via telephone lines. This storage scheme would make possible the evaluation of a variety of theoretical models by means of comparison with experimental data. Finally, there are areas of great interest in phototransport measurements that involve experiments on submicrosecond time scales and it would be beneficial to automate the data recording. We envisage, in the not too distant future, improvements of both hardware and software on

our system to aid us in achieving some or all of these enhanced performance characteristics.

Acknowledgments

The authors are indebted to D. C. Clarke and D. L. Raimondi for helpful programming advice. Thanks are due to D. E. Horne and H. Seki for conceiving many of the original experimental procedures. We express our special appreciation to D. E. Horne for the design and fabrication of most of the measurement instrumentation. W. D. Gill helped with the construction of the interface hardware and S. R. Heyer has been of great assistance in the operation of the automated experiments. We are grateful to Miss C. K. DeLong for her expert preparation of the manuscript.

References

1. N. P. Wilburn and L. D. Coffin, *IBM J. Res. Develop.* **13**, 46 (1969).
2. J. Frykland and W. Loveland, *IBM J. Res. Develop.* **13**, 75 (1969).
3. G. D. McCann, *IBM J. Res. Develop.* **13**, 28 (1969).
4. Y. Okaya, *IBM J. Res. Develop.* **13**, 126 (1969).
5. P. M. Grant, *IBM J. Res. Develop.* **15**, 293 (1971, this issue).
6. W. E. Spear, *J. Non-Crystalline Solids* **1**, 197 (1969).
7. I. P. Batra, B. H. Schechtman and H. Seki, *Phys. Rev. B*, **2**, 1592 (1970).
8. I. P. Batra and B. H. Schechtman, *J. Phys. Chem. Solids* **32**, 769 (1971).
9. H. Seki and I. P. Batra, *J. Appl. Phys.* **42**, 2407 (May 1971).
10. H. M. Gladney, *J. Comp. Phys.* **2**, 255 (1968); IBM Systems Reference Library Manuals A26-5918, C26-3703 and C26-3754.
11. P. M. Grant, *IBM J. Res. Develop.* **13**, 15 (1969).
12. H. Seki, *Phys. Rev. B*, **2**, 4877 (1970).
13. H. Seki, I. P. Batra, W. D. Gill, K. K. Kanazawa and B. H. Schechtman, *IBM J. Res. Develop.* **15**, 213 (1971).

Received November 25, 1970

The authors are located at the IBM Research Laboratory at San Jose, California 95114.